Investigating Earthquake Hazards in the Northern Salton Trough, Southern California, Using Data from the Salton Seismic Imaging Project (SSIP)

G. S. Fuis[1], J. A. Hole[2], J. M. Stock[3], N. W. Driscoll[4], G. M. Kent[5], A. J. Harding[4], A. Kell[5], M. R. Goldman[1], E. J. Rose[1], R. D. Catchings[1], M. J. Rymer[1], V. E. Langenheim[1], D. S. Scheirer[1], N. D. Athens[1], J. M. Tarnowski[6]

1 U.S. Geological Survey (USGS), Earthquake Science Center (ESC), Menlo Park, CA.

2 Virginia Polytechnic Institute and State University, Dept. Geosciences, Blacksburg, VA

3 California Institute of Technology, Seismological Laboratory 252-21, Pasadena, CA. .

4 Scripps Institution of Oceanography, La Jolla, CA.

5 Nevada Seismological Laboratory, University of Nevada, Reno, NV.

6 University of California, Riverside

Abstract

The southernmost San Andreas fault (SAF) system, in the northern Salton Trough (Salton Sea and Coachella Valley), is considered likely to produce a large-magnitude, damaging earthquake in the near future. The geometry of the SAF and the velocity and geometry of adjacent sedimentary basins will strongly influence energy radiation and strong ground shaking during a future rupture. The Salton Seismic Imaging Project (SSIP) was undertaken, in part, to provide more accurate information on the SAF and basins in this region.

We report preliminary results from modeling four seismic profiles (Lines 4-7) that cross the Salton Trough in this region. Lines 4 to 6 terminate on the SW in the Peninsular Ranges, underlain by Mesozoic batholithic rocks, and terminate on the NE in or near the Little San Bernardino or Orocopia Mountains, underlain by Precambrian and Mesozoic igneous and metamorphic rocks. These lines cross the Coachella Valley, which is underlain by Miocene to Holocene sedimentary deposits. Line 7 crosses the Salton Sea and sedimentary basin deposits to the northeast similar to those of the Coachella Valley. On three lines (7, 4, 6) there is evidence from our seismic imaging, potential-field studies, and (or) earthquakes that active strands of the SAF dip moderately NE.

From south to north, on Lines 7, 4, 5, and 6, maximum sedimentary basin depths are approximately 5.5?, 5.5, 3.5, and 3.5 km, respectively, as measured from the surface to the 5.3 km/s velocity contour. (In prior studies of the Imperial Valley, unmetamorphosed sediment is interpreted to lie above this approximate velocity contour [Kohler and Fuis, 1986].) Basement rocks that can be traced from the Peninsular Ranges to depth beneath the Coachella Valley are characterized by relatively high velocities, averaging 4.9 km/s at the surface and 6.4 km/s at a depth of 4 km. They are also characterized by high velocity gradients, averaging > 0.4/s. In contrast, rocks of the Little San Bernardino and Orocopia Mountains are characterized by relatively low velocities, averaging 3.9 km/s at the surface and 6.1 km/s at a depth of 4 km; and they are characterized by low velocity gradients, averaging < 0.4/s. The rocks of the Peninsular Ranges can be seen on Lines 4 and 6 extending at depth northeastward beyond the active surface trace(s) of the SAF.

Strong ground shaking from the ShakeOut Scenario Earthquake will be recalculated using our new non-vertical geometry for the SAF and new basin information.

Figure 1. Map showing extent of the Salton Seismic Imaging Project (SSIP). Seismic lines/arrays are labeled with numbers. (Line 1 is labeled in three segments--Line 1N, 1M, and 1S.)

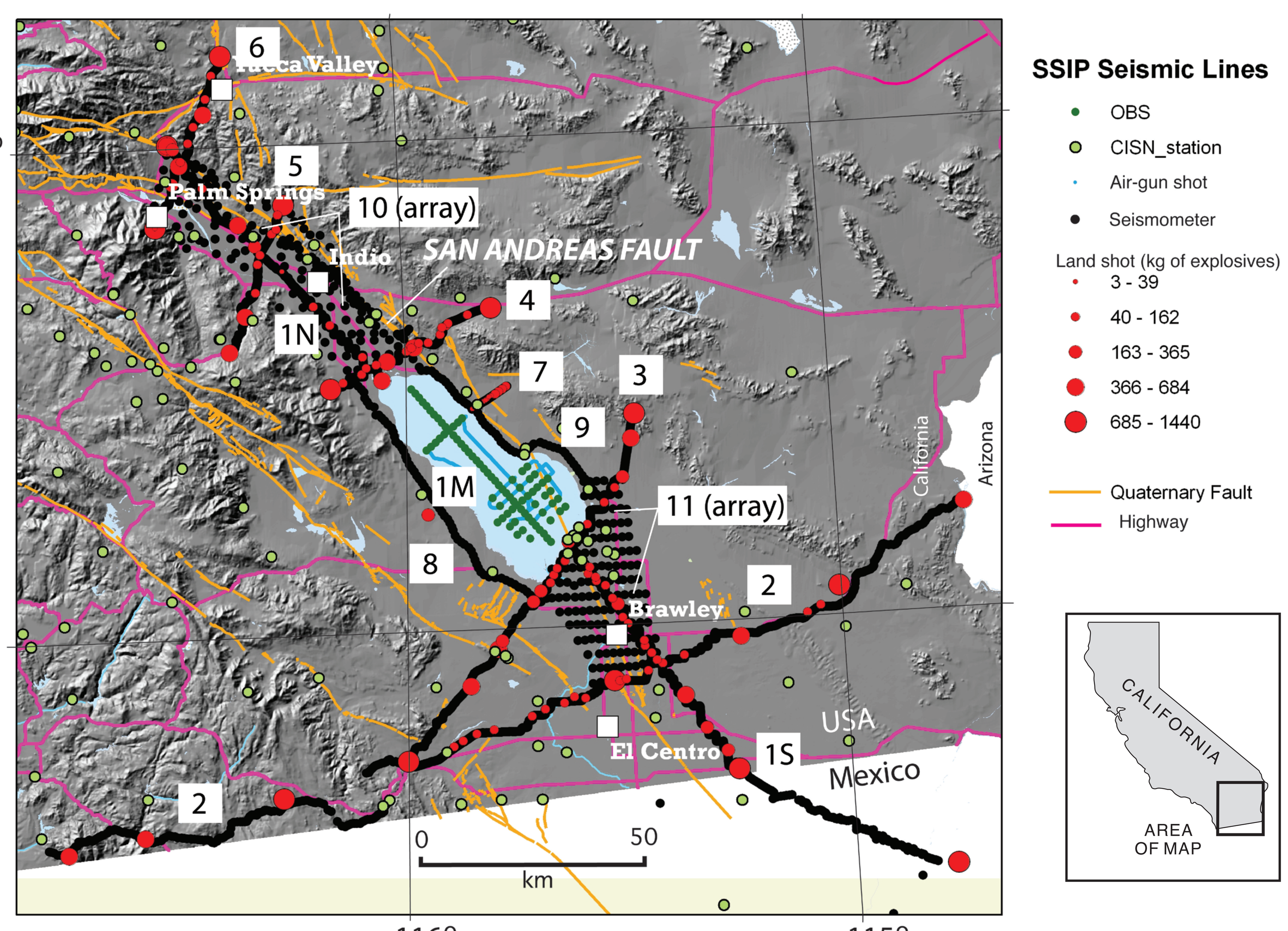

Refraction

Seismicity
Hauksson et al. (2012)
- 0.5 <= M < 3.0
- 3.0 <= M < 5.5
- 5.5 <= M

Mechanisms
Yang et al. (2012)
- M6
- M4
- M2

Line 6

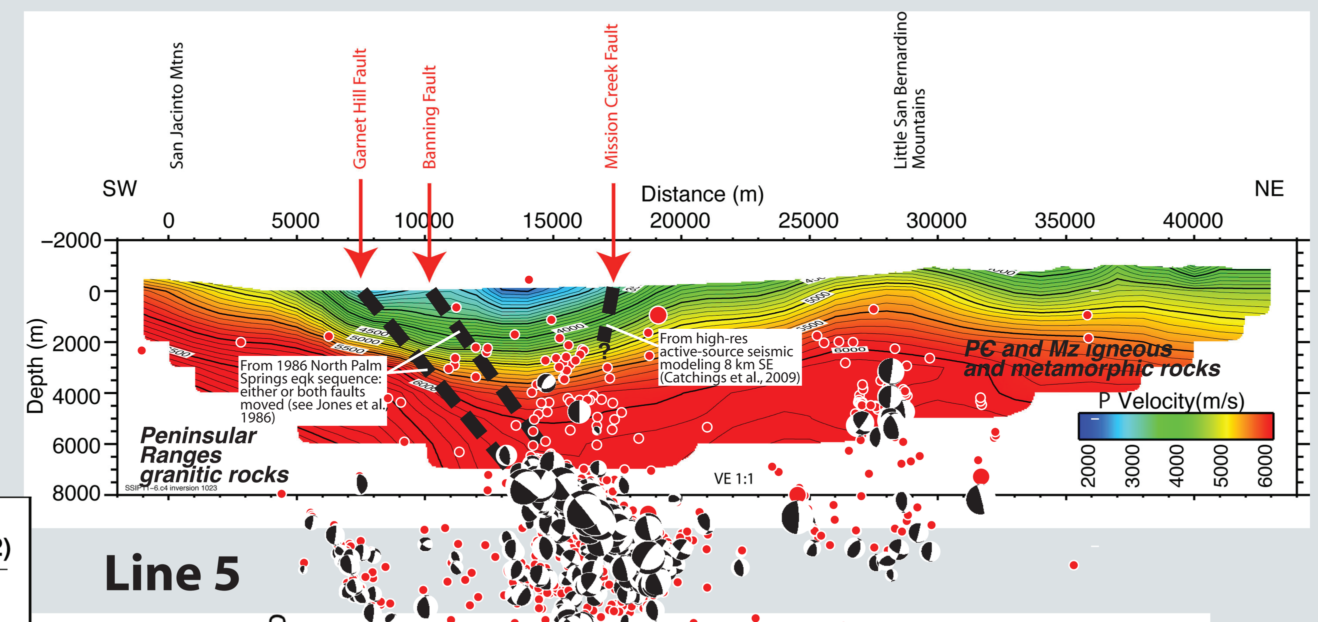

Line 5

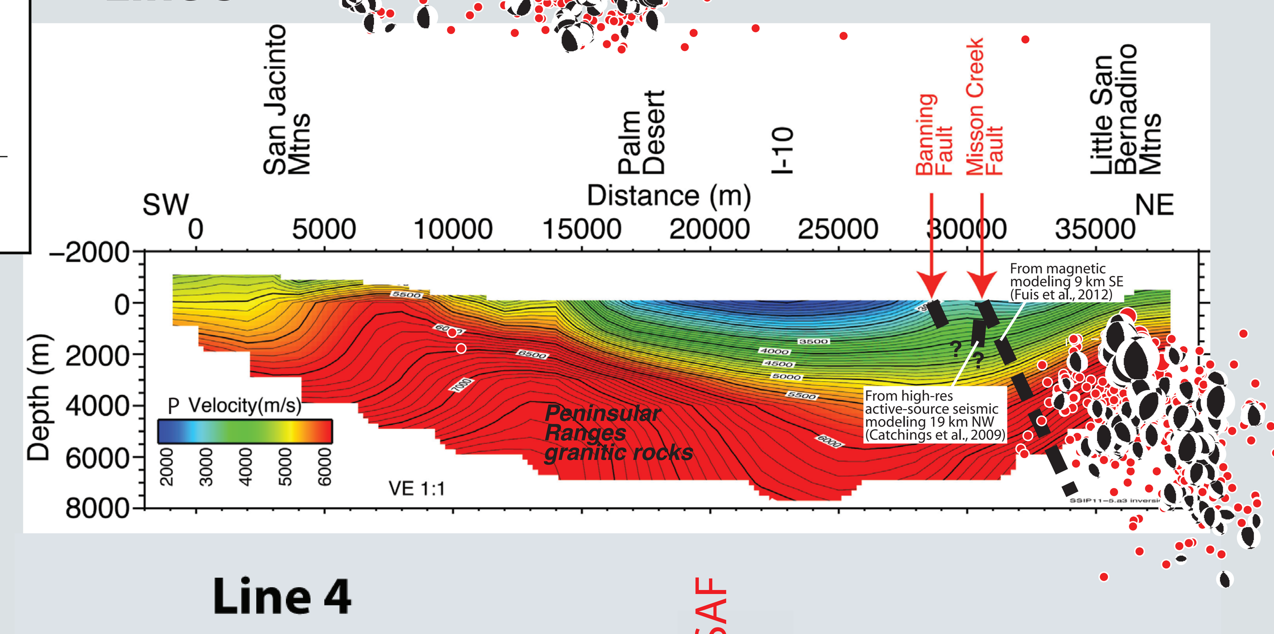

Line 4

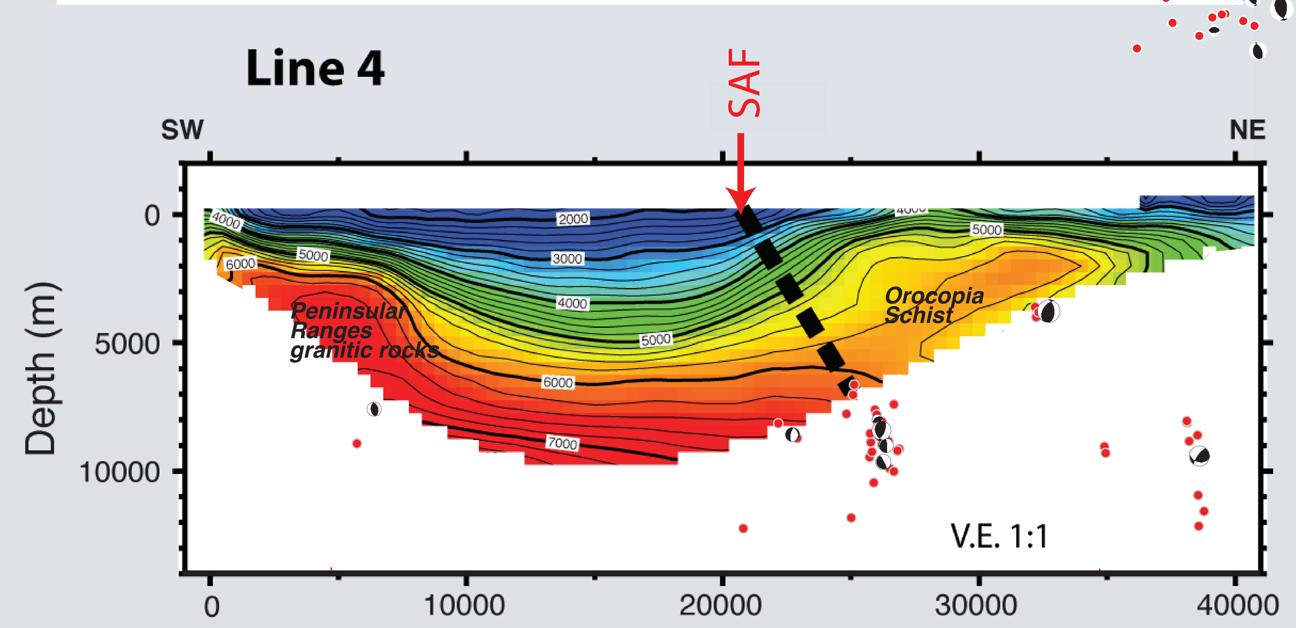

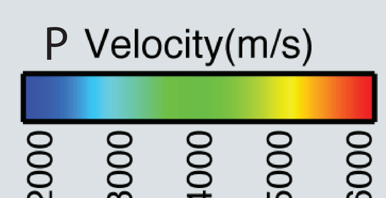

The tomographic velocity models in this column, and also in the next column, were obtained using the inversion algorithm of Hole (1992). Models for Lines 5 and 6 have not been fully tested using alternate starting velocity models, although alternate sets of picks have been used. The model for Line 4 has been more fully tested.

On Lines 4-6, we superpose earthquakes from Hauksson et al. (2012) and focal mechanisms from Yang et al. (2012); for Line 7, earthquakes from Lin et al. (2007). For all lines, projection distances are 2 km on either side of the cross sections.

The velocity models for Lines 4 and 6 are consistent with a NE dip for the active branches of the SAF, including the Garnet Hill and Banning faults on Line 6. This fault geometry separates rocks with relatively high velocities and high velocity gradients (Peninsular Ranges granitic rocks) from rocks with relatively low velocities and low velocity gradients (Precambrian and Mz igneous and metamorphic rocks in the Little San Bernardino Mts [Line 6] and Orocopia Schist in the Mecca Hills [Line 4]). Earthquakes alignments and focal mechanisms are also consistent with NE dips on these two lines. Red arrows point to surface traces of the San Andreas fault.

The velocity model for Line 5 shows no similar evidence for a NE dip. However, earthquakes may outline the hanging wall of a NE-dipping Mission Creek fault. Modeling of magnetic data 8 km SE of Line 5 does indeed indicate a moderate NE dip (Fuis et al., 2012). In contrast, high-res seismic imaging across the Mission Creek fault 19 km to the NW of Line 5 (and 8 km to the SE of Line 6) suggest a steep SW dip (Catchings et al., 2009). The Mission Creek fault is inactive northwestward of a point approximately 10 km NW of Line 5 (Pat Williams, oral commun., 2012).

Models

Line 7

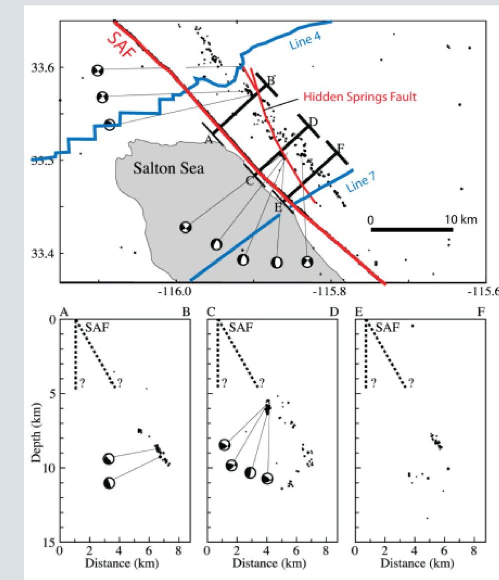

Figure 14 of Lin et al. (2007) with Lines 4 and 7 superposed. Dashed lines in the lower panel are alternative interpretations of the SAF.

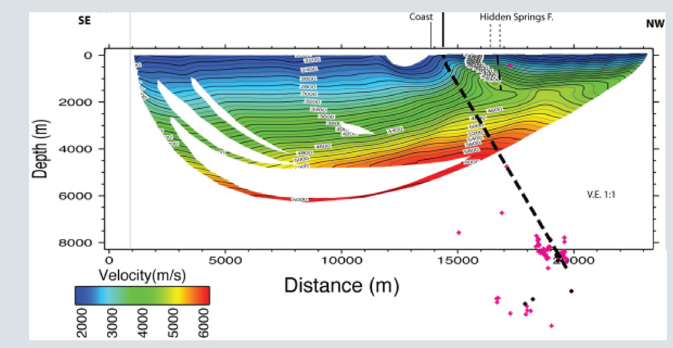

Model of Line 7 with earthquakes from above and interpretation of SAF superposed. Note that velocity contours in upper crust support a NE dip, as interpreted by Lin et al. (2007).

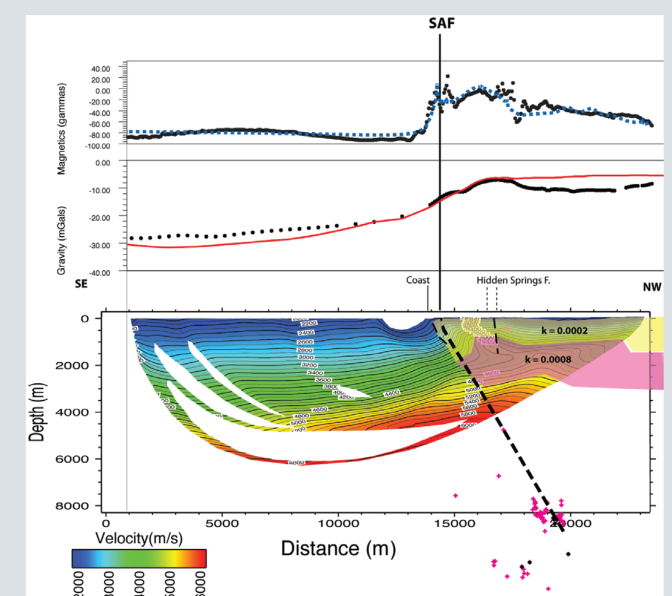

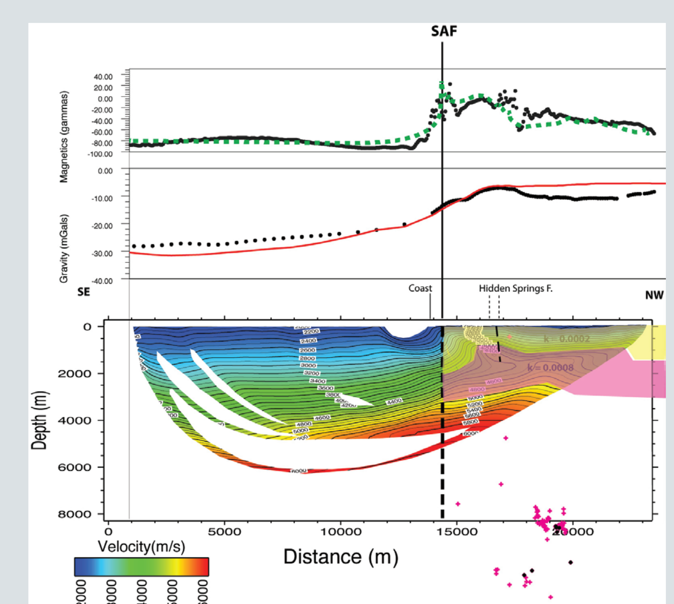

Observed (black dots) and calculated (colored lines) gravity and magnetic data are shown in these two panels, along with models of these data for two cases: dipping SAF (upper panel) and vertical SAF (lower panel). The dipping SAF is slightly favored by the magnetic data. [The magnetic data were collected on the ground and, offshore, in a boat.]

Reflection data

Line 7 (offshore part)

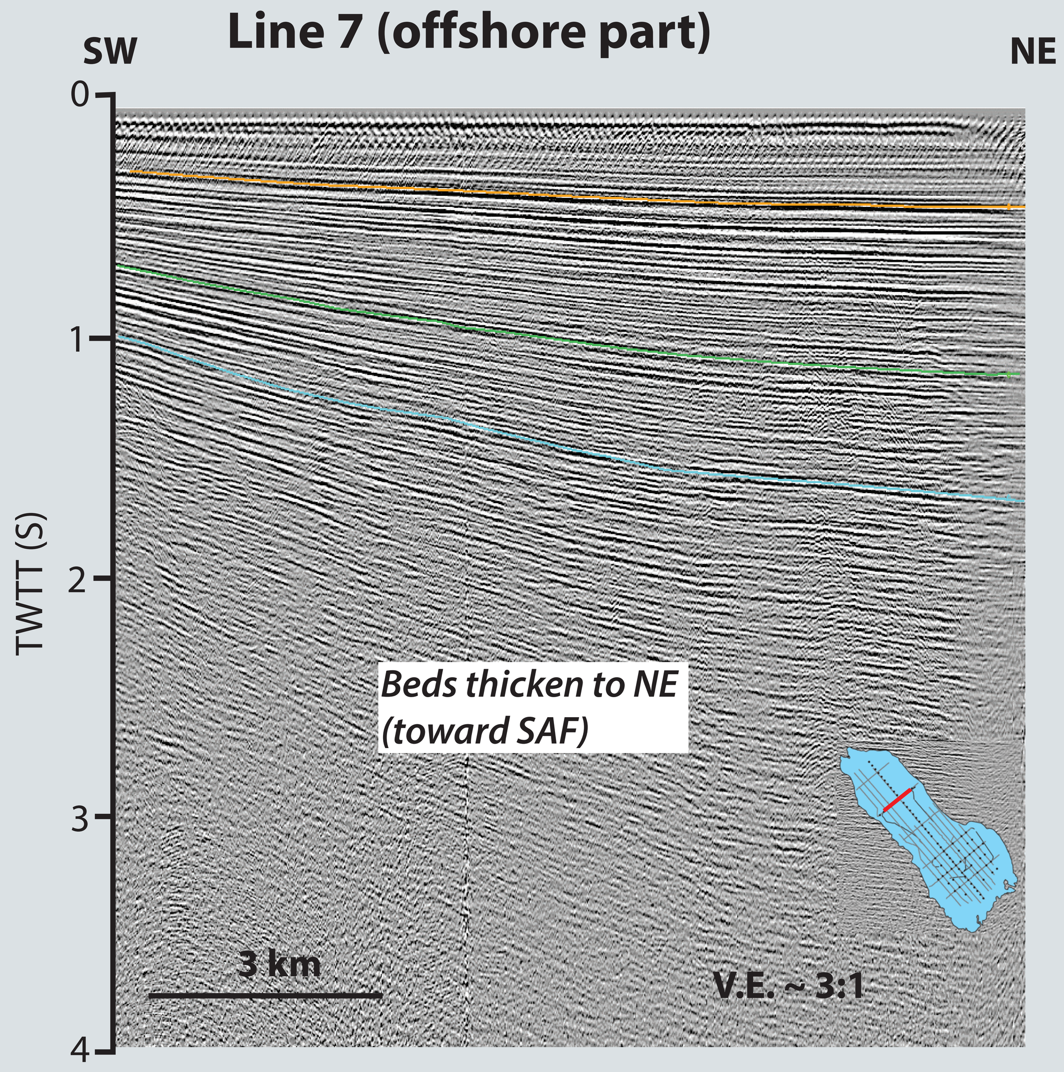

Line 1M (all offshore)

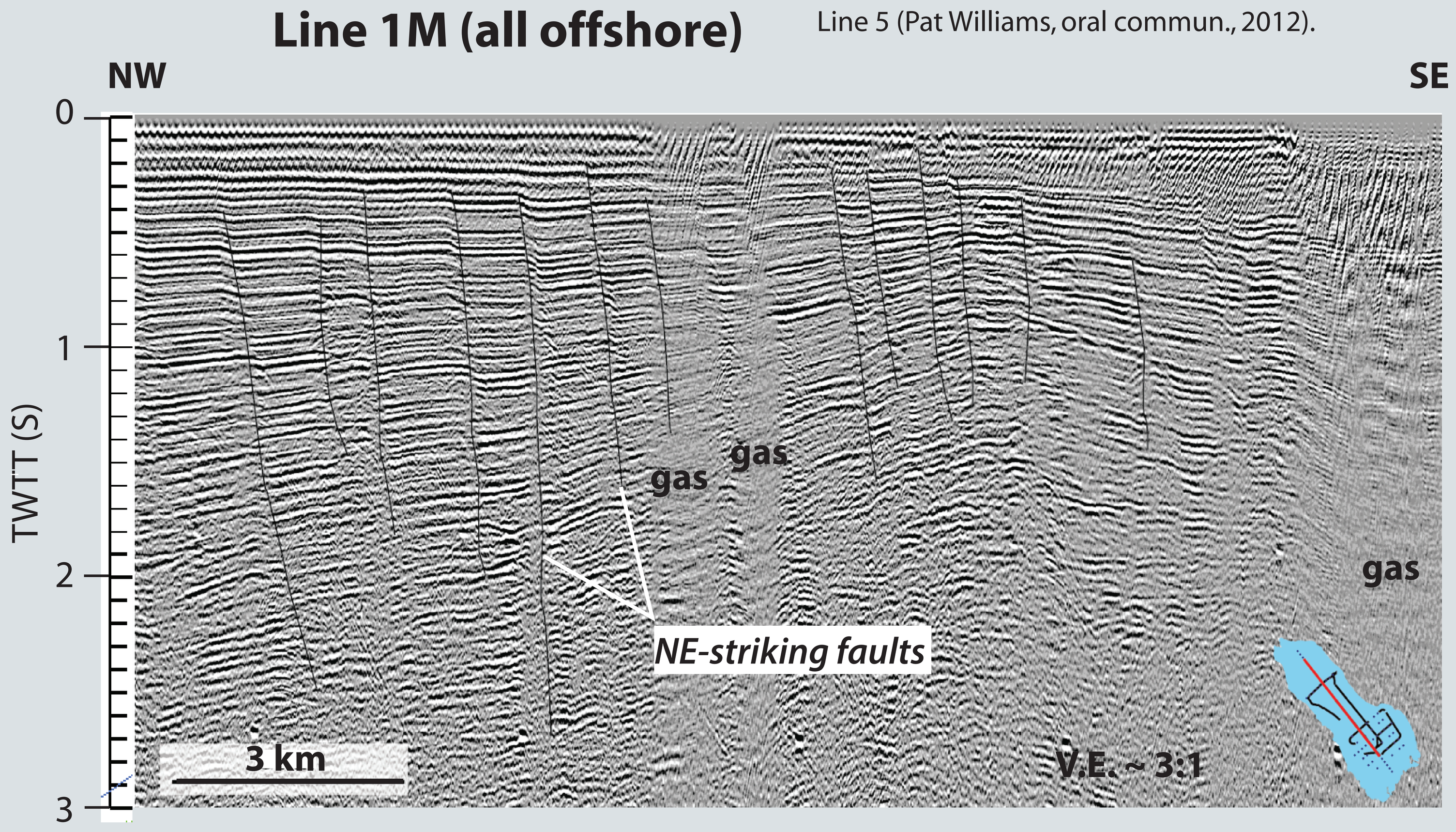

The panels above are reflection data recorded along two intersecting lines in the Salton Sea (see Figure 1 and insets). Airgun size was 210 cubic inches, except for the last day (90 cubic inches). Shot interval was 1 minute. The streamer was 300 m long and 48 channels. Reflection fold is 1-2 . Airgun signals were also recorded on 48 OBS's placed at 78 locations and on land seismometers (Texans and RT 130's). On Line 7 offshore, sedimentary beds dip and thicken northeastward toward the SAF. This type of structure is commonly seen where a normal fault bounds the sedimentary beds on the side toward which they dip and thicken. In this case, however, the northeastward dip and thickening may result from northwestward tilting of the Peninsular Ranges block , which underlies the Coachella Valley and the northern Salton Sea. Such tilting results from northwestward translation of the Pacific Plate against the "propeller"-shaped SAF of Fuis et al. (2012) (Michele Cooke and Laura Fattaruso, written comm., 2012).

REFERENCES:

Catchings, R.D., M.J. Rymer, M.R. Goldman, and G. Gandhok (2009). San Andreas fault geometry at Desert Hot Springs, California, and its effects on earthquake hazards and groundwater, *Bulletin Seismological Society America, 99,* 2190-2207.

Fuis, G.S., W.D. Mooney, J.H. Healy, G.A. McMechan, and W.J. Lutter (1984). A seismic refraction survey of the Imperial Valley region, California, *Journal Geophysical Research, 89,* p. 1165-1189.

Fuis, G.S., D.S. Scheirer, V.E. Langenheim, and M.D. Kohler (2012). A new perspective on the geometry of the San Andreas Fault in southern California and its relationship to lithospheric structure, *Bulletin Seismological Society America , 102,* p. 236-251.

Hauksson E., W. Yang and P. M. Shearer (2012). Waveform relocated earthquake catalog for southern California (1981 - 2011), *Bull. Seism. Soc. Am., 103-104*, in press.

Hole, J.A. (1992). Nonlinear high-resolution three-dimensional seismic travel time tomography, *Journal Geophysical Research, 97,* p. 6553-6562.

Jones, L.M., K. Hutton, D.D. Given, and C.R. Allen (1986). The North Palm Springs, California, earthquake equence of July 1986, *Bul letin Seismological Society America, 76,* 1830-1837.

Kohler, W.M., and G.S. Fuis (1986). Travel-time, time-term, and basement depth maps for the Imperial Valley region, California, from explosions, *Bulletin Seismological Society America, 76,* p. 1289-1303.

Lin, G., P.M. Shearer, and E. Hauksson (2007). Applying a three-dimensional velocity model, waveform cross-correlation, and clus ter analysis to locate southern California seismicity from 1981 to 2005, *Journal of Geophysical Research, 112,* B12309, doi:10/1029/2007JB004986.

Yang, W., E. Hauksson and P. M. Shearer (2012). Computing a Large Refined Catalog of Focal Mechanisms for Southern California (1981 – 2010): Temporal Stability of the Style of Faulting, *Bull. Seism. Soc. Am., 102,* 1179-1294.